arXiv:1509.01803v1 [cond-mat.quant-gas] 6 Sep 2015

Traveling Majorana solitons in a one-dimensional spin-orbit coupled Fermi superfluid

Peng Zou,[1] Joachim Brand,[2] Xia-Ji Liu,[1] and Hui Hu[1,*]
[1] *Centre for Quantum and Optical Science, Swinburne University of Technology, Melbourne 3122, Australia*
[2] *New Zealand Institute for Advanced Study, Centre of Theoretical Chemistry and Physics,*
and Dodd-Walls Centre for Photonic and Quantum Technologies, Massey University, Auckland, New Zealand

(Dated: September 8, 2015)

We investigate traveling solitons of a one-dimensional spin-orbit coupled Fermi superfluid in both topologically trivial and non-trivial regimes by solving the static and time-dependent Bogoliubov-de Gennes equations. We find a critical velocity v_h for traveling solitons that is much smaller than the value predicted using the Landau criterion due to the presence of spin-orbit coupling, which strongly upshifts the energy level of the soliton-induced Andreev bound states towards the quasi-particle scattering continuum. Above v_h, our time-dependent simulations in harmonic traps indicate that traveling solitons decay by radiating sound waves. In the topological phase, we predict the existence of peculiar Majorana solitons, which host two Majorana fermions and feature a phase jump of π across the soliton, irrespective of the velocity of travel. These unusual properties of Majorana solitons may open an alternative way to manipulate Majorana fermions for fault-tolerant topological quantum computations.

PACS numbers: 03.75.Lm, 67.85.Lm, 67.85.De

Solitons or localized waves that arise from the interplay between the dispersion and nonlinearity of underlying systems are fascinating phenomena occurring in many different fields of physics [1]. Over the past two decades, a major research emphasis has focused on solitons in atomic Bose-Einstein condensates (BECs) [2]. The family of BEC solitons consists of many interesting members, from bright solitons in attractive BECs [6] and gap solitons in optical lattices [7], to dark solitons in repulsively interacting BECs [3–5], which are created experimentally by imprinting a sharp and characteristic phase jump into the BEC. Remarkably, dark solitons may also be created in strongly interacting Fermi gases [8–16] at the crossover from BECs to Bardeen-Cooper-Schrieffer (BCS) superfluids [17], where phase kinks are encoded in the pairing order parameter. Their recent experimental observation may offer valuable insights into the nature of fermionic superfluidity in the strongly correlated regime [13, 18].

In this Letter, we consider traveling fermionic solitons in a different setup – one-dimensional (1D) Fermi superfluids with spin-orbit coupling (see Fig. 1) – and predict the existence of an exotic member of the soliton family when the superfluid becomes topologically non-trivial. It is referred to as Majorana soliton, owing to its ability to host two Majorana fermions that obey non-Abelian statistics at the soliton core [19, 20]. Majorana solitons are universal and remarkably robust, in the sense that their properties are not affected by a finite velocity of travel. In particular, the phase jump across a Majorana soliton is exactly pinned to π and the density profile is unchanged. In other words, Majorana solitons are not greyed by a finite velocity. This unique stability renders Majorana solitons an ideal platform to manipulate Majorana fermions for practical applications such as topological quantum computations [21].

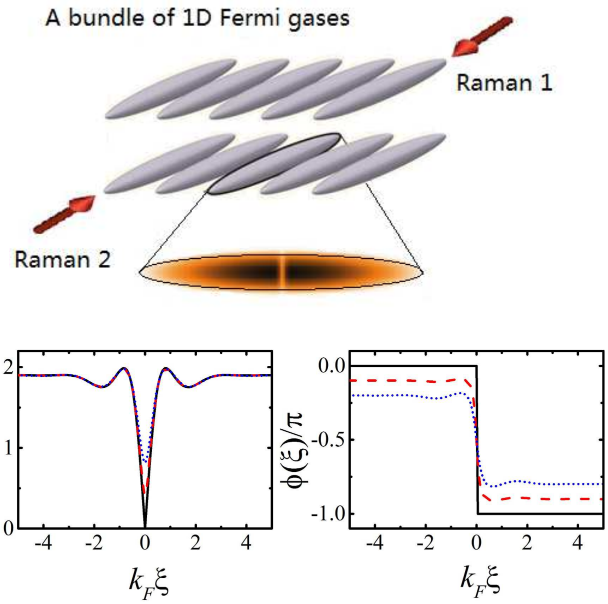

Figure 1: (color online). Upper panel: Sketch of the proposed experimental configuration. Many 1D tubes of spin-orbit coupled ^{40}K Fermi gases are formed using a 2D optical lattice and two counter-propagating Raman lasers. Lower panel: The magnitude $|\Delta(\xi)|$ and phase $\phi(\xi)$ of the soliton order parameter in the non-topological phase with parameters $\gamma = 3.41$, $h = 0.52E_F$ and $\lambda k_F/E_F = 1.71$. The solid, dashed and dotted lines correspond to soliton velocities $v_s = 0$, $0.15v_F$ and $0.3v_F$, respectively.

Our investigation is motivated by the recent realizations of spin-orbit coupling in atomic Fermi gases [22, 23] and the promising perspective of creating an atomic topological superfluid [24, 25]. Traveling Majorana solitons with fixed π phase step, if experimentally observed to oscillate inside a Fermi cloud, would be a smoking-gun proof of the existence of long-sought topological superfluids. We note that stationary dark solitons with Majorana fermions in a spin-orbit coupled Fermi gas were recently predicted [26, 27]. However, the crucial issue raised in any practical manipulations, i.e., the fate of these solitons at a finite velocity of motion, was not addressed.

Our results also suggest that a critical velocity for the stability of traveling solitons is greatly affected by spin-orbit coupling. This is because one of the mid-gap energy levels, the soliton-induced Andreev bound states (ABSs), is strongly up-shifted towards the bulk quasiparticle scattering continuum by spin-orbit coupling. As a result, the Andreev bound states are lost at a much smaller velocity v_h than the Landau critical velocity, which leads to a decay channel. At a velocity above v_h, we find that traveling solitons gradually decay via radiating sound waves.

Model. We start by describing a possible experimental configuration, as sketched in the upper panel of Fig. 1. A bundle of parallel, identical 1D spin-1/2 ^{40}K Fermi gases can be formed by adding a tight 2D optical lattice in the transverse $y-z$ plane [28], and the spin-orbit coupling with equal Rashba and Dresselhaus weight can be realized by adapting the so-called NIST scheme using two counter-propagating Raman laser beams [22]. The resulting 1D spin-orbit coupled Fermi gas in a single tube is modeled by the Hamiltonian $H = \int dx\, [\mathcal{H}_0 + \mathcal{H}_{\rm int}]$, where [24–27]

$$\mathcal{H}_0 = \left[\psi_\uparrow^\dagger(x), \psi_\downarrow^\dagger(x)\right] \left(\mathcal{H}_s + \lambda \hat{k}_x \sigma_y - h\sigma_z\right) \begin{bmatrix} \psi_\uparrow(x) \\ \psi_\downarrow(x) \end{bmatrix} \quad (1)$$

is the spin-orbit coupled single-particle part and

$$\mathcal{H}_{\rm int} = g_{\rm 1D} \psi_\uparrow^\dagger(x)\, \psi_\downarrow^\dagger(x)\, \psi_\downarrow(x)\, \psi_\uparrow(x) \quad (2)$$

with $g_{1D} < 0$ is the interaction Hamiltonian describing the attractive contact interaction between the two spin states ($\sigma = \uparrow, \downarrow$). Here, $\psi_\sigma^\dagger$ is the fermionic field operator that creates an atom with mass m in the spin state σ. The term $\lambda \hat{k}_x \sigma_y - h\sigma_z$ with the momentum operator $\hat{k}_x = -i\partial/\partial x$ and Pauli matrices σ_y and σ_z is induced by the Raman process, describing a synthetic spin-orbit coupling with strength $\lambda \equiv \hbar^2 k_R/m$ and an effective Zeeman field $h = \Omega_R/2$, where k_R and Ω_R are the momentum and Rabi frequency of the Raman beams [22], respectively. The term $\mathcal{H}_s = -\hbar^2\partial_x^2/(2m) + V_T(x) - \mu$ with the chemical potential μ describes the motion of atoms in a harmonic trapping potential $V_T(x) = m\omega^2 x^2/2$.

We solve the model Hamiltonian for stationary and traveling solitons within the mean-field approximation. This amounts to finding solutions with *phase-twisted* order parameter in the static and time-dependent Bogoliubov-de Gennes (BdG) equations, $\mathcal{H}_{\rm BdG}\mathbf{\Phi}_\eta(x) = E_\eta \mathbf{\Phi}_\eta(x)$ and $\mathcal{H}_{\rm BdG}\mathbf{\Phi}_\eta(x,t) = i\hbar(\partial/\partial t)\mathbf{\Phi}_\eta(x,t)$, respectively. Here, for convenience we have used the Nambu spinor representation and have introduced $\mathbf{\Phi}_\eta \equiv [u_{\uparrow\eta}, u_{\downarrow\eta}, v_{\uparrow\eta}, v_{\downarrow\eta}]^T$ and E_η as the wave-function and energy of Bogoliubov quasiparticles. The BdG Hamiltonian reads

$$\mathcal{H}_{\rm BdG} \equiv \begin{bmatrix} \mathcal{H}_s - h & -\lambda\partial/\partial x & 0 & -\Delta \\ \lambda\partial/\partial x & \mathcal{H}_s + h & \Delta & 0 \\ 0 & \Delta^* & -\mathcal{H}_s + h & \lambda\partial/\partial x \\ -\Delta^* & 0 & -\lambda\partial/\partial x & -\mathcal{H}_s - h \end{bmatrix}, \quad (3)$$

and the BdG equations, either static or time-dependent, should be self-consistently solved with the gap equation $\Delta = -(g_{1D}/2)\sum_\eta [u_{\uparrow\eta} v_{\downarrow\eta}^* f(E_\eta) + u_{\downarrow\eta} v_{\uparrow\eta}^* f(-E_\eta)]$ and the number equation $n = -(1/2)\sum_\eta [|u_{\sigma\eta}|^2 f(E_\eta) + |v_{\sigma\eta}|^2 f(-E_\eta)]$, where $f(E) = 1/(1+e^{E/k_B T})$ is the Fermi-Dirac distribution function and the summation is performed for the energy level (labeled by η) up to a high-energy cut-off E_c, i.e., $|E_\eta| < E_c$.

To obtain a moving soliton in a trapped gas, we first find a stationary dark soliton at x_0 away from the trap center [27]. By evolving such an initial state in time, the soliton is accelerated by the trap potential and caused to oscillate inside the Fermi cloud. The same procedure has previously been used to understand the dynamics of dark solitons in a BEC-BCS Fermi superfluid [9], and could also be employed in experiment.

We also search for traveling soliton solutions on a homogeneous (untrapped) background that satisfy $\Delta(x,t) = \Delta(x - v_s t) = \Delta(\xi)$, by solving the BdG equations in the co-moving frame with the velocity v_s [11]:

$$\mathcal{H}_{\rm BdG}(\xi)\mathbf{\Phi}_\eta(\xi) = \left[E_\eta - i\hbar v_s \frac{\partial}{\partial \xi}\right] \mathbf{\Phi}_\eta(\xi). \quad (4)$$

Here, $\mathcal{H}_{\rm BdG}(\xi)$ is obtained by replacing ∂_x with ∂_ξ and $\Delta(x,t)$ with $\Delta(\xi)$ in Eq. (3). In other words, we seek traveling solitons in a homogeneous gas that are stationary in the frame of the soliton. This technique provides more insights into the soliton properties and enables us to isolate effects caused by the trapping potential when we analyze time-dependent simulations [12]. For the calcuations in a box with length L we impose a modified periodic boundary condition, $\Delta(\xi + L/2) = \Delta(\xi - L/2)e^{i\delta\phi}$, to explicitly take into account a phase jump $\delta\phi$ across the soliton [16]. In addition, we implement a generalized secant (Broyden's) approach to make sure that the self-consistent iteration procedure will converge to a stable solution [11, 29].

In numerical calculations, we use a dimensionless interaction parameter to characterize the interaction strength, $\gamma = -mg_{1D}/(\hbar^2 n)$, which is basically the ratio between the interaction and kinetic energy at the density n. We choose the Fermi vector and energy, $k_F = \pi n/2$ and $E_F = \hbar^2 k_F^2/(2m)$, as the units of wave-vector and energy, respectively. For simulations in a trapped cloud with N atoms, it is convenient to use the peak density of a *non-interacting* Fermi gas in the Thomas-Fermi approximation at the trap center, $n' = (2/\pi)\sqrt{Nm\omega/\hbar}$,

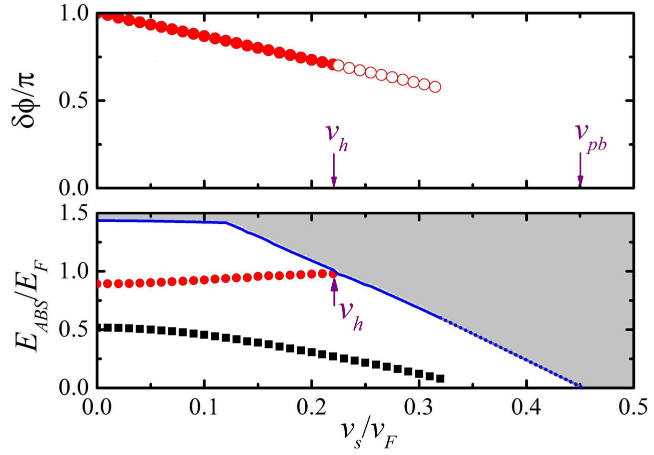

Figure 2: (color online). Upper panel: The phase jump $\delta\phi$ as a function of velocity in the non-topological phase. Lower panel: The corresponding mid-gap ABS energy levels. The arrows indicate the velocity v_h, at which the upper ABS (red circles) touches the quasi-particle scattering continuum (shadow area), and the pair-breaking velocity v_{pb}. Broyden's method fails to find traveling soliton solutions when the energy of the lower ABS is close to zero. Parameters are as in Fig. 1.

although the cloud itself is an interacting gas. We denote the corresponding units with k'_F and E'_F. Throughout this work, we consider only zero temperature. For trapped simulations we shall take the interaction parameter $\gamma \simeq 3$, spin-orbit coupling strength $\lambda k'_F/E'_F = 1.5$ and an energy cut-off $E_c = 10E'_F$. Parameters for homogeneous simulations are chosen to correspond to the relevant peak density of the interacting trapped gas.

There are two different regimes for a 1D spin-orbit-coupled Fermi superfluid [24, 25], depending on whether the effective Zeeman field h is over a threshold $h_c = \sqrt{\Delta^2 + \mu^2}$ ($\simeq E_F$ with our parameters for the trapped cloud). Once $h > h_c$, the superfluid becomes topologically non-trivial and hosts Majorana solitons. Before presenting our main results on Majorana solitons, it is useful to understand how traveling solitons are affected by spin-orbit coupling in the non-topological phase.

Non-topological phase. The spatial structure of the soliton order parameter in the nontopological phase ($h < h_c$) is illustrated in the lower panel of Fig. 1 for different soliton velocities. As the velocity increases, the dip in the order parameter profile becomes shallower, and its imaginary part develops structure and becomes larger at the soliton core. Consequently, the phase jump across the soliton decreases from π, as shown explicitly in the upper panel of Fig. 2. This turn-to-grey procedure of traveling solitons has been predicted earlier both for BEC-BCS crossover superfluids [11] and BECs [30, 31]. However, the presence of spin-orbit coupling leads to some interesting new features.

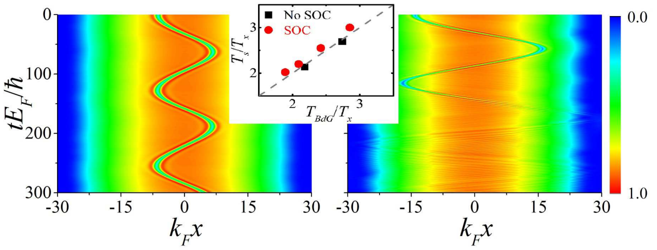

Figure 3: (color online). Time-dependent simulations of traveling solitons in a trapped, non-topological Fermi superfluid with $h = 0.4E'_F < h_c$. The color represents the magnitude of density (in units of n'). By choosing the initial position x_0, we generate two solitons, whose maximum velocity is $0.18v'_F < v_h = 0.22v'_F$ (left panel) and $0.42v'_F > v_h$ (right panel), respectively. The inset examines the universal relation (5) for the soliton oscillation period with/without spin-orbit coupling at different interaction strengths ($2.5 \leq \gamma \leq 3.2$). The period T_s from the time-dependent simulation is compared with T_{BdG} defined by the right hand side of Eq. (5) and calculated from the time-independent BdG solutions.

The most striking feature is that the mid-gap energy levels of soliton-induced ABSs now exhibit a pronounced velocity dependence, as seen from the lower panel of Fig. 2. Already at zero velocity, the ABS splits into two branches due to the combined effects of spin-orbit coupling and effective Zeeman field [26, 27]. With increasing the soliton velocity, the energy of the upper ABS gradually increases and merges into the quasi-particle scattering continuum at $v_h \simeq 0.22v_F$, which is much smaller than the pair-breaking velocity $v_{pb} \simeq 0.45v_F$. Any coupling between the upper ABS and the bulk continuum states [32] then will destroy the soliton-induced ABSs and in turn make the soliton unstable. Thus, we anticipate that the soliton may decay when its velocity is beyond the threshold v_h, for example, by dissipating its energy in the form of sound waves.

We have checked this conjecture by performing time-dependent simulations in harmonic traps, as reported in Fig. 3. By carefully selecting the position x_0 of the initially stationary dark soliton, the maximum velocity v_m - reached when the traveling soliton passes the trap center - can be tuned. For $v_m < v_h$, we find a stable oscillation of the traveling soliton (see the left panel). The oscillation period T_s seems to satisfy the elegant universal relation (see the inset),

$$\left(\frac{T_s}{T_x}\right)^2 = \frac{M^*}{M} = 1 + \frac{\hbar n}{2M}\frac{d\left(\delta\phi\right)}{dv_s}, \tag{5}$$

which was derived by treating soliton as a classical particle [9, 31]. Here, $T_x = 2\pi/\omega$ is the trapping period, M and M^* are respectively the physical and inertial mass of the soliton and their difference is proportional to the derivative of the phase jump [9]. In contrast, at $v_m > v_h$, the soliton gradually spreads out in the density profile and after a few periods we see only low-amplitude den-

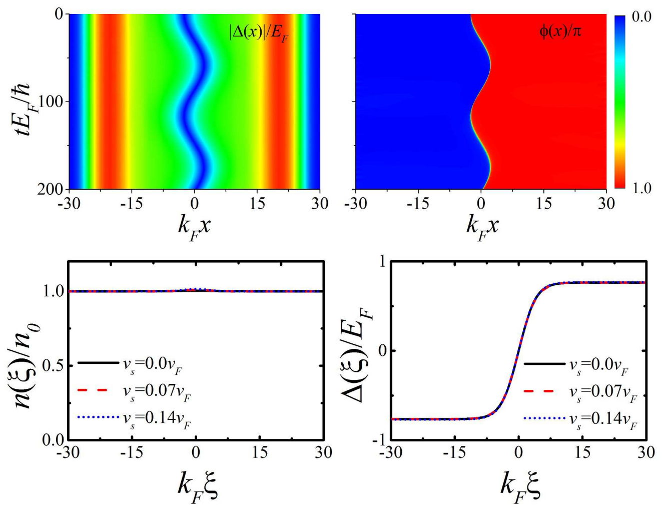

Figure 4: (color online). Majorana soliton. The two upper panels report the time evolution of the magnitude $|\Delta(x,t)|$ (left) and the phase $\phi(x,t)$ (right) of the order parameter for a Majorana soliton in a trapped topological Fermi superfluid ($h = 1.2E'_F > h_c$) with a maximum soliton velocity $0.07v_F < v_h$. The two lower panels show the density (left) and order parameter (right) of a Majorana soliton in the homogeneous configuration at different velocities with parameters $\gamma = 3.75$, $h = 1.71E_F$ and $\lambda k_F/E_F = 1.79$.

sity ripples (right panel). By examining the speed of these ripples, we identify them as sound waves. Our time-dependent simulations with spin-orbit coupling therefore indicate that the critical velocity of traveling solitons could be significantly smaller than Landau critical velocity v_{pb}, which was found to be the relevant critical velocity without spin-orbit coupling [9–11]. These result are still consistent, since without spin-orbit coupling v_h actually is close to the pair-breaking velocity [12].

Topological phase. By increasing effective Zeeman field across $h_c \simeq E_F$ for a trapped Fermi cloud, the local energy gap (and hence the pair-breaking velocity) at the trap center closes and then re-opens. A topological superfluid emerges.The first sign of the existence of a velocity-independent Majorana soliton comes from the time-dependent simulations in harmonic traps, as shown in the upper panel of Fig. 4. During the time evolution, the dip minimum in $|\Delta(x,t)|$ remains at zero and the phase jump $\delta\phi(t)$ across the soliton is always pinned at π (see also the inset in Fig. 5). In the lower panel of Fig. 4, we check more rigorously the velocity dependence using Broyden's approach. With increasing the soliton velocity in the topological phase, the density and pairing order parameter profiles remain essentially unchanged.

To show the presence of Majorana fermions at the soliton core, we report in Fig. 5 the energy of the ABS as a function of the traveling velocity. Although in the co-moving frame the energy E^{Mov}_{ABS} increases (linearly) with the velocity, the energy in the laboratory frame, $E^{\rm Lab}_{ABS}$,

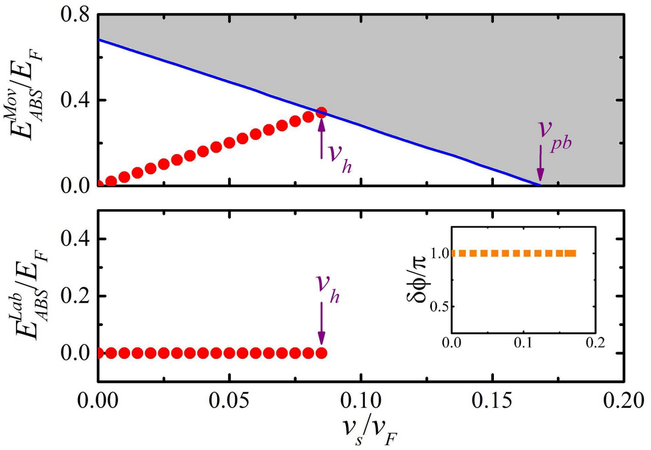

Figure 5: (color online). The ABS energy of the Majorana soliton as a function of the soliton velocity in the co-moving frame (upper panel) or in the laboratory frame (lower panel). We note that in the topological phase, the number of the ABS states decreases to one [27], if we count only positive energy levels. The inset examines the π-phase of Majorana solitons. Parameters as in Fig. 4.

which is related to the co-moving energy by

$$E^{\rm Lab}_{ABS} = E^{\rm Mov}_{ABS} + \int d\xi \mathbf{\Phi}^*_{ABS}(-i\hbar v_s)\partial\mathbf{\Phi}_{ABS}/\partial\xi, \quad (6)$$

is precisely zero [33]. This is expected behavior for a Majorana fermion, which must have zero energy due to the particle-antiparticle symmetry. Together with the observed continuity with the zero velocity case [26, 27], we conclude that the moving soliton in the topological phase indeed hosts Majorana fermions.The properties of the Majorana soliton at finite velocity can be made plausible from the universal relation (5), if we assume its validity in the topological phase. We recall that the density notch in Majorana solitons is absent [26, 27] and hence the physical mass vanishes [9]. Equation (5) immediately implies that the derivative of the phase jump is zero, since the oscillation period should be finite. This leads to a constant π phase jump, irrespective of the soliton velocity. In turn, the magnitude of order parameter should vanish at the soliton core.

It is worth noting that Eq. (5) can hardly be used to predict the oscillation period of Majorana solitons, as the ratio between zero mass and zero derivative of the phase jump is undetermined. How to amend the universal relation for Majorana solitons needs further exploration. For a large velocity, we find a similar situation as in the non-topological case (see the upper panel of Fig. 5). Naïvely, we anticipate that Majorana solitons may cease to exist once $v_s > v_h$. However, time-dependent simulations in traps suggest that the instability via emitting sound waves occurs at a very long time scale, presumably due to the weak coupling between the ABS and quasi-particle continuum. This again indicates the robustness of Majorana solitons.

Experimental observation of Majorana solitons. The proposed experimental scheme in Fig. 1 is easy to set up [22, 28], although the realization of 1D topological superfluids is difficult due to the lack of efficient cooling techniques [22]. Majorana solitons can be created by imprinting a sharp phase jump [13, 15]. The observation of their oscillations seems to be an experimental challenge, as the density profile of Majorana solitons remains flat [26, 27]. One then has to measure the local pairing order parameter. A suitable detection technique is the spatially resolved radio-frequency spectroscopy [34], which may give information about the local order parameter, provided that the size of Majorana solitons is comparable with the spatial resolution of spectroscopy.

Conclusions and outlook. We have predicted the existence of an exotic member to the soliton family - the Majorana soliton - which may exist universally in any 1D topological superfluids including p-wave superfluids and semiconductor/superconductor nanowire structures [35]. Our results may also be applicable to 2D topological superfluids. In that case, it would be interesting to examine the possibility of finding a moving vortex that is able to host a single Majorana fermion in the vortex core. In analogy to Majorana solitons, the properties of such a vortex would be insensitive to its velocity.

We are grateful to Franco Dalfovo, Robin Scott and Yan-Hua Hou for fruitful discussions. This research was supported by the Marsden Fund of New Zealand (contract number UOO1320) and by the ARC Discovery Projects (FT130100815, DP140100637, DP140103231 and FT140100003).

---

[*] Electronic address: hhu@swin.edu.au

[1] P. G. Drazin and R. S. Johnson, Solitons: *An Introduction* (Cambridge University Press, Cambridge, England, 2002).

[2] P. G. Kevrekidis, D. J. Frantzeskakis, and R. Carretero-Gonzláez, *Emergent Nonlinear Phenomena in Bose-Einstein Condensates, Theory and Experiement* (Springer, New York, 2007).

[3] S. Burger, K. Bongs, S. Dettmer, W. Ertmer, K. Sengstock, A. Sanpera, G. V. Shlyapnikov, and M. Lewenstein, Phys. Rev. Lett. **83**, 5198 (1999).

[4] B. P. Anderson, P. C. Haljan, C. A. Regal, D. L. Feder, L. A. Collins, C. W. Clark, and E. A. Cornell, Phys. Rev. Lett. **86**, 2926 (2001).

[5] C. Becker, S. Stellmer, P. S.-Panahi, S. Dörscher, M. Baumert, E.-M. Richter, J. Kronjäger, K. Bongs, and K. Sengstock, Nature Phys. **4**, 496 (2008).

[6] J. Denschlag, J. E. Simsarian, D. L. Feder, C. W. Clark, L. A. Collins, J. Cubizolles, L. Deng, E. W. Hagley, K. Helmerson, W. P. Reinhardt, S. L. Rolston, B. I. Schneider, and W. D. Phillips, Science **287**, 97 (2000).

[7] E. A. Ostrovskaya and Y. S. Kivshar, Phys. Rev. Lett. **90**, 160407 (2003).

[8] M. Antezza, F. Dalfovo, L. P. Pitaevskii, and S. Stringari, Phys. Rev. A **76**, 043610 (2007).

[9] R. G. Scott, F. Dalfovo, L. P. Pitaevskii, and S. Stringari, Phys. Rev. Lett. **106**, 185301 (2011).

[10] A. Spuntarelli, L. D. Carr, P. Pieri, and G. C. Strinati, New J. Phys. **13**, 035010 (2011).

[11] R. Liao and J. Brand, Phys. Rev. A **83**, 041604 (2011).

[12] R. G. Scott, F. Dalfovo, L.P. Pitaevskii, S. Stringari, O. Fialko, R. Liao, and J. Brand, New J. Phys. **14**, 023044 (2012).

[13] T. Yefsah, A. T. Sommer, M. J. H. Ku, L. W. Cheuk, W. Ji, W. S. Bakr, and M. W. Zwierlein, Nature (London) **499**, 426 (2013).

[14] A. Bulgac, M. M. Forbes, M. M. Kelley, K. J. Roche, and G. Wlazlowski. Phys. Rev. Lett. **112**, 025301 (2014).

[15] M. J. H. Ku, W. Ji, B. Mukherjee, E. Guardado-Sanchez, L. W. Cheuk, T. Yefsah, and M. W. Zwierlein, Phys. Rev. Lett. **113**, 065301 (2014).

[16] D. K. Efimkin and V. Galitski, Phys. Rev. A **91**, 023616 (2015).

[17] S. Giorgini, L. P. Pitaevskii, and S. Stringari, Rev. Mod. Phys. **80**, 1215 (2008).

[18] M. J. H. Ku, B. Mukherjee, T. Yefsah, and M. W. Zwierlein, arXiv:1507.01047 (2015).

[19] E. Majorana, Nuovo Cimento **14**, 171 (1937).

[20] F. Wilczek, Nature Phys. **5**, 614 (2009).

[21] C. Nayak, S. Simon, A. Stern, M. Freedman, and S. Das Sarma, Rev. Mod. Phys. **80**, 1083 (2008).

[22] P. Wang, Z.-Q. Yu, Z. Fu, J. Miao, L. Huang, S. Chai, H. Zhai and J. Zhang, Phys. Rev. Lett. **109**, 095301 (2012).

[23] L. W. Cheuk, A. T. Sommer, Z. Hadzibabic, T. Yefsah, W. S. Bakr, and M. W. Zwierlein, Phys. Rev. Lett. **109**, 095302 (2012).

[24] X.-J. Liu and H. Hu, Phys. Rev. A **85**, 033622 (2012).

[25] R. Wei and E. J. Mueller, Phys. Rev. A. **86**, 063604 (2012).

[26] Y. Xu, L. Mao, B. Wu, and C. Zhang, Phys. Rev. Lett. **113**, 130404 (2014).

[27] X.-J. Liu, Phys. Rev. A **91**, 023610 (2015).

[28] Y.-A. Liao, A. S. C. Rittner, T. Paprotta, W. Li, G. B. Partridge, R. G. Hulet, S. K. Baur, and E. J. Mueller, Nature (London) **467**, 567 (2010).

[29] A. Baran, A. Bulgac, M. M. Forbes, G. Hagen, W. Nazarewicz, N. Schunck, and M. V. Stoitsov, Phys. Rev. C **78**, 014318 (2008).

[30] T. Tsuzuki, J. Low Temp. Phys. **4**, 441 (1971).

[31] V. V. Konotop and L. Pitaevskii, Phys. Rev. Lett. **93**, 240403 (2004).

[32] Broyden's approach does not capture such a coupling and can predict traveling soliton solutions at $v_s > v_h$.

[33] Due to the particle-hole symmetry, there is another ABS branch whose energy decreases linearly with the traveling velocity in the co-moving frame. In the lab frame, its energy is also precisely zero, giving rise to another Majorana fermion hosted by the Majorana soliton.

[34] Y. Shin, C. H. Schunck, A. Schirotzek, and W. Ketterle, Phys. Rev. Lett. **99**, 090403 (2007).

[35] V. Mourik, K. Zou, S. M. Frolov, S. R. Plissard, E. P. A. M. Bakkers, and L. P. Kouwenhoven, Science **336**, 1003 (2012).